Journal of Applied Ecology

Extending full protection inside existing multiple-use marine protected areas or reducing fishing effort outside can both deliver conservation and fisheries outcomes

Journal:	*Journal of Applied Ecology*
Manuscript ID	Draft
Manuscript Type:	Research Article
Date Submitted by the Author:	n/a
Complete List of Authors:	Belharet, Mokrane; Politecnico di Milano, Di Franco, Antonio; Universite de Nice Sophia Antipolis UFR Sciences, Calò, Antonio; Université Côte d'Azur; Università di Palermo Dipartimento di Scienze della Terra e del Mare Mari, Lorenzo; Politecnico di Milano, Claudet, Joachim; National Center for Scientific Research, CRIOBE; Casagrandi, Renato; Politecnico di Milano Gatto, Marino; Politecnico di Milano, Dipartimento di Elettronica, Informazione e Bioingegneria Lloret, Josep; Universitat de Girona, Sève, Charlotte; National Center for Scientific Research, PSL Université Paris, CRIOBE, USR3278 CNRS-EPHE-UPVD, Maison des Océans Guidetti, Paolo; Université Côte d'Azur, CNRS, UMR 7035 ECOSEAS, Parc Valrose 28, Melià, Paco; Politecnico di Milano Dipartimento di Elettronica Informazione e Bioingegneria,
Key-words:	Fisheries management, Metapopulation models, Coastal fish, Stock assessment, Marine conservation, Marine protected areas, Sustainable fisheries

Extending full protection inside existing multiple-use marine protected areas or reducing fishing effort outside can both deliver conservation and fisheries outcomes

Mokrane Belharet[1], Antonio Di Franco[2,3], Antonio Calò[2,4,5], Lorenzo Mari[1], Joachim Claudet[6], Renato Casagrandi[1], Marino Gatto[1], Josep Lloret[7], Charlotte Sève[6], Paolo Guidetti[2], Paco Melià[1]

[1]Dipartimento di Elettronica, Informazione e Bioingegneria, Politecnico di Milano, Via Ponzio 34/5, 20133 Milano, Italy.

[2]Université Côte d'Azur, CNRS, UMR 7035 ECOSEAS, Parc Valrose 28, Avenue Valrose, 06108 Nice, France.

[3]Stazione Zoologica "Anton Dohrn" sede interdipartimentale di Palermo, Italy

[4]CoNISMa, Piazzale Flaminio 9, 00196 Roma, Italy.

[5]Dipartimento di Scienze della Terra e del Mare (DiSTeM), Università di Palermo, Via Archirafi 20, 90123 Palermo, Italy

[6]National Center for Scientific Research, PSL Université Paris, CRIOBE, USR3278 CNRS-EPHE-UPVD, Maison des Océans, 195 rue Saint-Jacques 75005 Paris, France.

[7]University of Girona, Faculty of Science, C/Maria Aurèlia Company 69, 17003 Girona, Catalonia, Spain.

Correspondence

Mokrane Belharet

E-mail: mokrane.belharet@gmail.com

Paco Melià

E-mail: paco.melia@polimi.it

Running head: Full protection helps rebuild fish stocks

Word count: 6071 (summary: 268; main text: 3546; acknowledgements: 66; references: 1688; figure legends: 301); tables: 0; figures: 5; references: 47

Abstract

1 Most fish stocks worldwide are overfished, and many fisheries management strategies have failed to achieve sustainable fishing. Identifying effective fisheries management strategies has now become urgent.

2 Here, we developed a spatially-explicit metapopulation model accounting for seascape connectivity in the Mediterranean Sea, and parameterized it for three ecologically and economically important coastal fish species: *Diplodus sargus*, *Diplodus vulgaris* and *Epinephelus marginatus*.

3 We used the model to assess how stock biomass and catches respond to changes in fishing mortality rate (F) and in the size of fully protected areas within the existing network of multiple-use marine protected areas (MPAs). For each species, we estimated maximum sustainable yield (MSY) and the corresponding values of stock biomass (B_{MSY}) and fishing mortality rate (F_{MSY}), providing crucial reference points for the assessment of fisheries management.

4 All three species are currently overexploited. Stock recovery to B_{MSY} requires a reduction of current F between 25–50% (depending on the species). This would guarantee an increase in both stock biomass (17–42%) and catch (2–13%) after a transient time of ~10–20 years. Alternatively, increasing the size of fully protected areas over fishable areas within the existing network of MPAs would lead to positive conservation effects for all three species without impairing the productivity and profitability of the fishery.

5 *Synthesis and applications.* We provide the first assessment of stock status for three coastal species in the north-western Mediterranean and evaluate the ecological and fisheries outcomes of different management strategies. Extending full protection inside

existing multiple-use marine protected areas and/or reducing fishing effort outside can both deliver conservation and fisheries outcomes.

Key words

Fisheries management, Metapopulation models, Coastal fish, Stock assessment, Marine conservation.

1 Introduction

Marine fisheries provide a major source of food and livelihood for hundreds of millions of people worldwide (FAO 2018). However, most of the world's fish stocks are overfished (Costello *et al.* 2016), with strong cascading impacts on both marine biodiversity (Sala *et al.* 2012; Ortuño Crespo & Dunn 2017) and societies (Golden *et al.* 2016).

Several strategies have been proposed to pursue sustainability in fisheries (Hoggarth 2006; Coll *et al.* 2013; Goetze *et al.* 2016; Carvalho *et al.* 2019). Traditional management has focused on adjusting fishing effort to levels guaranteeing maximum sustainable yield (MSY), i.e. the maximum catch that can be removed from a stock over time without depleting it. MSY and its related biological reference points, such as stock biomass (B_{MSY}) and fishing mortality rate (F_{MSY}), are benchmarks used for gauging the status of a stock or fisheries (Hilborn & Ovando 2014). Although many coastal species are key targets for small scale artisanal and recreational fisheries (Lloret *et al.* 2019), for most of them these reference points have never been assessed.

In coastal areas, multiple-use Marine Protected Areas (MPAs) can be used as a means to combine maritime spatial planning and the ecosystem approach to fisheries management (Claudet *et al.* 2006; Gaines *et al.* 2010; Melià *et al.* 2016). Their actual ecological effectiveness is affected by the presence and extent of fully protected areas within MPA borders (Zupan *et al.* 2018). Although they are often not established primarily for fisheries management (García-Charton *et al.* 2008), MPAs can provide benefits to fisheries (Russ & Alcala 2004; Di Franco *et al.* 2016) and other socioeconomic activities (Pascual *et al.* 2016). Finding a balance between biological conservation and socioeconomic viability is fundamental to ensure the consensus among stakeholders necessary for the success of MPAs (Klein *et al.* 2013; Melià 2017).

Whether benefits at the local scale (thanks to recruitment subsidy and/or spillover effects; Di Lorenzo *et al.* 2016) can scale-up and make MPAs useful tools for fisheries management also at a broader scale is still controversial (Hilborn 2015; Hughes *et al.* 2016). Quantitative tools

able to describe the coupled spatiotemporal dynamics of fish and fisheries are hence crucial to assess the actual implications of proposed management measures in a realistic way (Botsford *et al.* 2009; Bastardie *et al.* 2017). Although studies linking seascape connectivity with population dynamics are scarce to date (but see, e.g., Watson *et al.* 2012; Treml *et al.* 2015), the explicit integration of these aspects into a metapopulation approach is key to understand the ecological and evolutionary dynamics of coastal marine populations, as well as to assess the long-term consequences of alternative management policies from a spatially explicit perspective (Botsford *et al.* 2009; Guizien *et al.* 2014).

Here we developed two sets of scenarios to assess the role of MPA networks as a tool to support fisheries management of three key coastal species in the north-western Mediterranean Sea. The scenarios were simulated using a biophysical metapopulation model, based on realistic patterns of connectivity estimated via Lagrangian simulations. The performances of each scenario were evaluated in terms of three indicators of conservation and socioeconomic relevance: stock biomass, fisheries catch and total value of catch. First, we tested the effects of regulating fishing mortality rates and estimated biological reference points for the three species. Second, we tested the role of the presence and size of fully protected areas in determining the bio-economic effectiveness of multiple-use MPAs. Finally, we discussed the effectiveness of the considered scenarios for achieving sustainable fisheries management objectives.

2 Methods

2.1 Case study

The study area covers the north-western Mediterranean Sea, and in particular the region located between latitudes 38.5°N– 45°N and longitudes 1°E–12°E. We focused on three fish species of high ecological and economic relevance (Guidetti *et al.* 2014) and vulnerable to small scale and recreational fishing (Lloret *et al.* 2019): the white seabream *Diplodus sargus*, the two-banded

seabream *Diplodus vulgaris*, and the dusky grouper *Epinephelus marginatus*. The three species are common in the Mediterranean Sea: they thrive in littoral rocky bottoms and generally occur from a few meters down to approximately 50 m depth, although they can be found, at lower densities, even at greater depths (especially *E. marginatus*; Harmelin & Harmelin-Vivien 1999). Their bipartite life cycle is typical of the majority of coastal species, with a pelagic larval phase and a benthic adult phase (see section S1 in the Supplementary Information for further details).

2.2 Metapopulation model

We developed an age-structured, discrete-time metapopulation model, based on a biophysical model accounting for habitat suitability and oceanographic connectivity. The model describes, in a spatially explicit framework, all the key biological processes affecting the species' demographic dynamics, such as reproduction, larval dispersal, recruitment, and natural and fishing mortality. In the following sections, we concisely summarize the main features of the model; further details about its structure and formulation are given in section S2, while details on its calibration and validation are given in section S3.

2.2.1 Habitat suitability

The selected fish species have very similar habitat requirements. Therefore, we assumed the same suitable habitat (rocky and hard substrate, including coralligenous assemblages between 0–50 m depth) for all three species. Habitat was mapped using available information on bathymetry and seabed habitats from the EMODnet portal (www.emodnet.eu). Bathymetry was provided as a high-resolution raster map (1/480°; Populus et al. 2017). Seabed habitat maps were hand-corrected in QGIS software; in fact, although EMODnet maps represent the most updated georeferenced seafloor maps for the Mediterranean Sea, some areas included in our domain were associated to low confidence levels, while others completely lacked any habitat

132 information. For these areas, we first cross-checked information on the EMODnet map with the
133 distribution of coastline substrate types reported in Furlani *et al.* (2014), and then we analysed
134 high-resolution satellite images from Google Earth to ascertain substrate type where the
135 information did not match. In case of mismatch or absence of habitat information in the original
136 map, we added a buffer of rocky substrate along the coast with its extent inversely proportional
137 to the sea bottom slope.

138 **2.2.2 Connectivity assessment**

139 To evaluate seascape connectivity among local populations (i.e. among model cells), we carried
140 out Lagrangian simulations of larval dispersal across the study area with an individual-based
141 biophysical model. The physical component of the model was based on daily average current
142 velocity fields made available through the Copernicus Marine Environment Monitoring Service
143 (marine.copernicus.eu). Velocity fields, produced by the Mediterranean Sea physics reanalysis
144 (Fratianni *et al.* 2014), had a 1/16° (~6–7 km) horizontal resolution and covered 72 unevenly
145 spaced vertical levels. Lagrangian particles were released according to the reproductive
146 schedule of each species and tracked for the duration of the whole larval phase. Simulations
147 covered a 12-year-long time horizon (2004–2015). Results were aggregated across a grid with
148 the same resolution of the ocean circulation dataset (1/16°) and used to derive a set of
149 connectivity matrices for each species and each year. The element $c_{\{i,j,t\}} = \frac{n_{i \to j,t}}{n_{i,t}}$ of the
150 connectivity matrix $C(t)$ is the ratio between $n_{i \to j,t}$ (i.e. the number of larvae starting from
151 source cell i and successfully arriving to destination cell j at the end of their pelagic larval
152 duration in year t) and $n_{i,t}$ (i.e. the total number of propagules released from cell i in year t).
153 The diagonal elements of each connectivity matrix represent the retention rates of the
154 considered cells in a specific year.

2.2.3 Protection

To describe the protection regime of each marine area, we considered three levels of protection: unprotected, partially protected and fully protected areas. Each cell within the spatial domain of the model was associated with at least one protection level. When there was more than one protection level in the same cell, we calculated the relative coverage of each protection level with respect to the total surface of the cell. To this end, we considered the 62 nationally designated Marine Protected Areas (MPAs) already established in the study area. Some are fully protected areas and some are multiple-use MPAs containing a fully protected area (Horta e Costa *et al.* 2016). Partially protected areas were identified with the portion of MPA that is not fully protected. Information on the MPAs (geographical coordinates, names, areas, establishment year, presence of fully protected areas, etc.) was derived from the MAPAMED database (medpan.org/main_activities/mapamed/). MPA perimeters were provided as georeferenced polygons, allowing us to define the geometric intersection with each cell and to calculate the corresponding surface area.

2.2.4 Population dynamics

Metapopulation dynamics were described by subdividing the stocks of the three species into subpopulations according to the same horizontal grid used for the connectivity assessment. To account for the heterogeneous distribution of suitable habitat within the study area, each cell was further subdivided into 30×30 sub-cells matching the spatial resolution of the bathymetric grid. The marine surface area A_i of each cell i was evaluated as the sum of the areal extent of its sub-cells with a valid bathymetric value. For each cell i**,** we calculated the surface area of suitable habitat A_i^{SH} as the area of the geometric intersection between the portion of cell between 0–50 m depth and the polygon of the suitable substrate. Only the cells with non-zero A_i^{SH} score (949 cells in total) were included in the metapopulation model (Fig. 1). Each sub-population was subdivided into age classes (15 for *D. sargus*, 9 for *D. vulgaris* and 20 for *E. marginatus*),

whose dynamics were described by taking into account both the local demographics and the exchange of larvae under the action of the currents.

2.3 Fisheries management scenarios

Once calibrated and validated, we used the model to test different fisheries management scenarios for the three model species at the scale of the whole study area. Specifically, we investigated the response of stock biomass and catch to changes in (i) the fishing mortality rate, and (ii) the extent of fully protected areas in the current network of MPAs. In the first set of experiments, we considered a homogeneous reduction or increase of current fishing mortality rate (F_0) across the study area. In the second set of experiments, we changed the relative coverage of existing fully protected areas in the MPAs currently established in the study area, keeping the total surface area of each MPA unchanged. The area not included in the fully protected area was considered to be partially protected (i.e. with an intermediate level of fishing mortality).

For each management scenario, we performed a 50-year-long simulation with a time-averaged connectivity matrix and assuming the present distribution of the three metapopulations (as reconstructed through the calibration of the model) as the initial condition. The last ten years of each simulation were used to assess stock biomass and catch (integrated across space and averaged over time) for each species.

To evaluate the economic implications of the different scenarios tested, we estimated also the total value of catch (TVC) obtained from the fishery of the three study species. TVC was calculated as $\sum_k p_k \overline{C_k}$, where p_k is the market price of species k, and $\overline{C_k}$ is the total catch of species k averaged over the last 10 years of simulation. The relative change of TVC for each scenario was expressed as a percent change with respect to the TVC of the baseline simulation. Market prices were considered, based on an informal ex-vessel survey carried out across the

study area, to be 20 EUR/kg for *D. sargus*, 18 EUR/kg for *D. vulgaris*, and 25 EUR/kg for *E. marginatus*.

3 Results

3.1 Effects of changing fishing mortality rate

The responses of stock biomass and catch of the three studied species to changes of fishing mortality rate at the scale of the whole study area are shown in Fig. 2. To make species-specific results easier to compare, we normalized biomass and catch values for each species with respect to the baseline simulation (performed under current fishing mortality, as estimated *via* model calibration). For all three species, normalized maximum sustainable yield (MSY) and the corresponding normalized stock biomass are >1, indicating that there is room for improvement over current management. Indeed, fishing mortality rates associated with MSY (F_{MSY}) are lower than current fishing mortality (F_0) for all species ($0.75F_0$ for *D. sargus*, and $0.5F_0$ for *D. vulgaris* and *E. marginatus*), suggesting that all three stocks are presently overfished.

For *D. sargus,* baseline biomass (B_0) and catch (C_0) are 83% and 98% of B_{MSY} and MSY, respectively. For the other two species, the discrepancy is even more pronounced: B_0 and C_0 for *D. vulgaris* are 64% and 90% of those associated with F_{MSY}, while for *E. marginatus* they are 58% and 87%, respectively. The relative values of B_{MSY} compared to unfished biomasses (i.e. with fishing effort set to zero across the whole study area) are 41% (for *D. sargus*), 47% (for *D. vulgaris*) and 37% (for *E. marginatus*). In parallel, the ratio of baseline biomass (B_0) on unfished biomass is 34% for *D. sargus*, 30% for *D. vulgaris*, and 22% for *E. marginatus*.

Fig. 3A shows the temporal dynamics of stock biomass over time under an MSY scenario. At the beginning of the simulations, relative biomass B/B_{MSY} is 0.85 for *D. sargus*, 0.61 for *D. vulgaris* and 0.60 for *E. marginatus*. Subsequently, relative biomass grows progressively until reaching its maximum ($B/B_{MSY} = 1$). The duration of the transient required to approach B_{MSY}

(i.e. for a full recovery of the stock) is ~10–20 years for the three species. Fig. 3B shows the temporal dynamics of catch (expressed, in this case, as the ratio between current catch and its present value, C/C_0) under the same scenario (MSY). Relative catches fall, during the first year of implementation of the scenario, from the present level (= 1 by definition) to approximately 0.79 for *D. sargus,* 0.55 for *D. vulgaris* and 0.54 for *E. marginatus*. Afterwards, they grow over time until reaching their maximum value (1.02 for *D. sargus*, 1.11 for *D. vulgaris* and 1.15 for *E. marginatus*). The time required to attain the present levels again ($C/C_0 = 1$) is about 16 years for *D. sargus*, 11 years for *D. vulgaris* and 10 years for *E. marginatus*.

3.2 Effects of expanding fully protected areas

Predicted responses of stock biomass and catch of the three species to changes in the relative coverage of fully protected areas (keeping fishing mortality rate at its present level F_0) are shown in Fig. 4. The effect of expanding fully protected areas on fish biomass are positive for all species and approximately proportional to the extent of full protection. When the relative coverage of full protection is set to 100% of the total protected area, the predicted increase in stock biomass relative to the baseline is 33% for *D. sargus*, 40% for *D. vulgaris*, and 61% for *E. marginatus*. On the other hand, effects on catch are species-dependent. For *D. sargus* and *E. marginatus*, catch is negatively related to the fully protected fraction (except when this ranges between its current value and 10% of the total protected area). In contrast, for *D. vulgaris* the effect of increasing the fully protected fraction is generally positive, except when the fraction is lower than the present one or >90% of the total protected area. In particular, catch of *D. vulgaris* is expected to be maximized by a fully protected area ~40% of the total protected area.

3.3 Economic consequences of the analysed scenarios

The response of total value of catch to changes in fishing mortality is shown in Fig. 5A. Under the current protection scheme, the predicted change in the total value of catch is positive for *F*

252 comprised between $0.4F_0$ and F_0. The maximum value (+8%) is achieved for a fishing mortality
253 ~60% of the present one. Beyond its maximum, total value declines progressively with
254 increasing fishing mortalities.
255 The effect of changing the extent of full protection within existing MPAs on the total value of
256 catch are shown in Fig. 5B. The maximum value (+0.5%) is achieved when the fraction of fully
257 protected area is equal to 20%. Benefits are positive when the fraction ranges between the
258 current value (8%) and 30%, and become negative outside this interval.

259 4 Discussion

260 We showed that the stocks of the three studied fish species (*Diplodus sargus*, *D. vulgaris* and
261 *Epinephelus marginatus*) are currently overexploited in the north-western Mediterranean, and
262 that fisheries sustainability could be reached either by reducing significantly fishing mortality
263 in unprotected areas or by increasing the size of fully protected areas while keeping fishing
264 constant.
265 Estimated current stock biomasses (B_0) are lower than B_{MSY} for the three studied species.
266 However, the level of depletion ($B_0 > 0.5B_{MSY}$ for all species) is such that all three species, and
267 in particular *D. sargus*, have a good chance of recovery and avoid collapse if fishing pressure
268 is reduced rapidly and substantially (Neubauer *et al.* 2013).
269 Achieving MSY requires that fishing mortality rates be significantly reduced (by one quarter
270 for *D. sargus* and one half for *D. vulgaris* and *E. marginatus*). In practice, this could be achieved
271 through a range of management tools including both input (e.g. gear restrictions, reduction of
272 fishing capacity) and output controls (e.g. reduction in allowable catch). Additionally, we show
273 that in the medium/long term (10–20 years), such a prospect of fishery recovery would
274 simultaneously generate increases in stock biomass (17–42% depending upon species),

fisheries catch (2–13%) and, consequently, revenues for the fishery sector (8% of increase in the total value of catch).

While the positive effects on stock biomass of the three studied species would be visible immediately after starting the recovery plan, our simulations suggest that the process of rebuilding catch to levels at least equal to the current ones would take more time (16 years for *D. sargus*, 11 years for *D. vulgaris* and 10 years for *E. marginatus*). During this relatively long transient period, catches may be substantially reduced, especially in the first year (about –20% for *D. sargus* and –45% for *D. vulgaris* and *E. marginatus*). To avoid excessive socioeconomic impacts (Worm *et al.* 2009) or unreported or illegal fishing (Agnew *et al.* 2009), specific measures should be targeted towards fishers during this transient period.

Enforcement of fishing effort control in unprotected areas may be difficult to put into practice, especially in the case of small scale and recreational fisheries in coastal areas. Therefore, an effective alternative strategy could be to rely on already designated MPAs and extend the coverage of full protection within the existing MPA network. Increasing the relative size of fully protected areas within multiple-use MPAs, while keeping fishing mortality rate outside MPAs at current levels, can generate positive conservation effects (increase in stock biomass) for the three coastal species. Positive effects of the size of fully protected areas on fish biomass are known (Claudet *et al.* 2008) and can be related to better inclusion of fish home ranges (Di Franco *et al.* 2018) and increase in self-recruitment through larger proportions of retained larvae (Botsford, Micheli & Hastings 2003).

Benefits on catch are species-specific and dependent on the size of the fully protected area. In our case, they are greater for the species with the longest dispersal distance (*D. vulgaris*) than for those with a narrower dispersion range (*D. sargus* and *E. marginatus*). Given that the three studied coastal species have limited adult movement (La Mesa *et al.* 2011; Di Franco *et al.*

2018), the relatively short pelagic larval phase represents the primary opportunity for dispersal and connectivity (Di Franco *et al.* 2012; Andrello *et al.* 2013; Pujolar *et al.* 2013).

Ensuring that the loss in fishing grounds is offset by gains in catch (Halpern & Warner 2003; Gaines *et al.* 2010) is key for successful fisheries management with MPAs. Here, we showed that an increase of size of fully protected areas within existing multiple-use MPAs can generate positive effects for *D. sargus* and *D. vulgaris*, both in terms of stock biomass (+2% and +15%, respectively) and catch (+0.5% and +4%, respectively), for levels of full protection between 10% and 40%, respectively, of the total protected area. In the case of *E. marginatus,* increasing the relative size of the fully protected area would not generate positive effects on catch. However, given that adult spillover was not taken into account in this study, the actual benefits on catch may be underestimated. In any case, the economic viability of the fishery (expressed in terms of total value of catch) would be preserved.

Despite the ecological and commercial interests of the studied coastal species, to our knowledge our study is the first modelling effort of its kind, fully integrating the biological and demographic characteristics of the species into a single model. We have shown that strong conservation benefits can be obtained either through non-spatial regulations, by reducing fishing effort in unprotected areas, or via area-based management strategies, by increasing the size of fully protected areas within existing MPAs (hence not increasing the size of MPAs overall). We believe this can contribute greatly to more effective management of those vulnerable species and help reconcile conservation and fisheries goals (Halpern et al. 2010).

Authors' contributions

PM and MB conceived the ideas and designed methodology. MB developed and ran the models, with support from PM, LM, MG and RC. ADF, AC and PG contributed in acquisition and

interpretation of data. MB led the writing of the manuscript. All authors contributed critically to the drafts and gave final approval for publication.

Acknowledgements

The present work has been carried out in the framework of the SafeNet project, funded by the European Commission, Directorate General for Maritime Affairs and Fisheries (grant SI2.721708 "Marine protected areas: network(s) for enhancement of sustainable fisheries in EU Mediterranean waters" (MARE/2014/41)). Additional funding came from the European Union's Horizon 2020 research and innovation programme (grant 641762 "ECOPOTENTIAL: Improving future ecosystem benefits through Earth observations").

References

Agnew, D.J., Pearce, J., Pramod, G., Peatman, T., Watson, R., Beddington, J.R. & Pitcher, T.J. (2009) Estimating the worldwide extent of illegal fishing. *Plos One*, **4**, e4570.

Andrello, M., Mouillot, D., Beuvier, J., Albouy, C., Thuiller, W. & Manel, S. (2013) Low connectivity between Mediterranean marine protected areas: a biophysical modeling approach for the dusky grouper *Epinephelus marginatus*. *Plos One*, **8**, e68564.

Bastardie, F., Angelini, S., Bolognini, L., Fuga, F., Manfredi, C., Martinelli, M., Nielsen, J.R., Santojanni, A., Scarcella, G. & Grati, F. (2017). Spatial planning for fisheries in the Northern Adriatic: working toward viable and sustainable fishing. *Ecosphere*, **8**, e01696.

Botsford, L.W., Micheli, F. & Hastings, A. (2003) Principles for the design of marine reserves. *Ecological Applications*, **13**, 25–31.

Botsford, L.W., White, J.W., Coffroth, M.-A., Paris, C.B., Planes, S., Shearer, T.L., Thorrold, S.R. & Jones, G.P. (2009) Connectivity and resilience of coral reef metapopulations in marine protected areas: matching empirical efforts to predictive needs. *Coral Reefs*, **28**, 327–337.

Carvalho, P.G., Jupiter, S.D., Januchowski-Hartley, F.A., Goetze, J., Claudet, J., Weeks, R., Humphries, A., White, C. (2019). Optimized fishing through periodically harvested closures. *Journal of Applied Ecology* (in press).

Claudet, J., Osenberg, C.W., Benedetti-Cecchi, L., Domenici, P., García-Charton, J., Pérez-Ruzafa, Á., Badalamenti, F., Bayle-Sempere, J., Brito, A. & Bulleri, F. (2008) Marine reserves: size and age do matter. *Ecology letters*, **11**, 481–489.

Claudet, J., Roussel, S., Pelletier, D. & Rey-Valette, H. (2006) Spatial management of near shore coastal areas: The use of Marine Protected Areas (MPAs) in a fisheries management context. *Life and Environment*, **56**, 301–305.

Coll, M., Cury, P., Azzurro, E., Bariche, M., Bayadas, G., Bellido, J.M., Chaboud, C., Claudet, J., El-Sayed, A.F., Gascuel, D., Knittweis, L., Pipitone, C., Samuel-Rhoads, Y., Taleb, S., Tudela, S. & Valls, A. (2013). The scientific strategy needed to promote a regional ecosystem-based approach to fisheries in the Mediterranean and Black Seas. *Reviews in Fish Biology and Fisheries*, **23**, 415–434.

Costello, C., Ovando, D., Clavelle, T., Strauss, C.K., Hilborn, R., Melnychuk, M.C., Branch, T.A., Gaines, S.D., Szuwalski, C.S., Cabral, R.B., Rader, D.N. & Leland, A. (2016) Global fishery prospects under contrasting management regimes. *Proceedings of the National Academy of Sciences*, **113**, 5125–5129.

Di Franco, A., Coppini, G., Pujolar, J.M., De Leo, G.A., Gatto, M., Lyubartsev, V., Melià, P., Zane, L. & Guidetti, P. (2012) Assessing Dispersal Patterns of Fish Propagules from an effective Mediterranean Marine Protected Area. *Plos One*, **7**, e52108.

Di Franco, A., Plass-Johnson, J.G., Di Lorenzo, M., Meola, B., Claudet, J., Gaines, S.D., García-Charton, J.A., Giakoumi, S., Grorud-Colvert, K., Hackradt, C.W., Micheli, F. &

Guidetti, P. (2018) Linking home ranges to protected area size: The case study of the Mediterranean Sea. *Biological Conservation*, **221**, 175–181.

Di Franco, A., Thiriet, P., Di Carlo, G., Dimitriadis, C., Francour, P., Gutiérrez, N.L., Jeudy de Grissac, A., Koutsoubas, D., Milazzo, M., Otero, M. del M., Piante, C., Plass-Johnson, J., Sainz-Trapaga, S., Santarossa, L., Tudela, S. & Guidetti, P. (2016) Five key attributes can increase marine protected areas performance for small-scale fisheries management. *Scientific Reports*, **6**, 38135.

Di Lorenzo, M., Claudet, J. & Guidetti, P. (2016) Spillover from marine protected areas to adjacent fisheries has an ecological and a fishery component. *Journal for Nature Conservation*, **32**, 62–66.

FAO (2018) *The State of World Fisheries and Aquaculture 2018. Meeting the sustainable development goals*. FAO, Rome.

Fratianni, C., Simoncelli, S., Pinardi, N., Cherchi, A., Grandi, A. & Dobricic, S. (2015). "Mediterranean RR 1955-2015 (Version 1) ". [Data set]. Copernicus Monitoring Environment Marine Service (CMEMS).

Furlani, S., Pappalardo, M., Gómez-Pujol, L. & Chelli, A. The rock coast of the Mediterranean and Black sea. *Geological Society, London, Memoirs*, **40**, 89–123.

Gaines, S.D., White, C., Carr, M.H. & Palumbi, S.R. (2010) Designing marine reserve networks for both conservation and fisheries management. *Proceedings of the National Academy of Sciences*, **107**, 18286–18293.

García-Charton, J.-A., Pérez-Ruzafa, Á., Marcos, C., Claudet, J., Badalamenti, F., Benedetti-Cecchi, L., Falcón, J.M., Milazzo, M., Schembri, P.J., Stobart, B., Vandeperre, F., Brito, A., Chemello, R., Dimech, M., Domenici, P., Guala, I., Le Diréach, L., Maggi, E. & Planes, S. (2008). Effectiveness of European Atlanto-Mediterranean MPAs: do they accomplish the expected effects on populations, communities and ecosystems? *Journal for Nature Conservation*, **16**, 193–221.

Goetze, J., Langlois, T., Claudet, J., Januchowski-Hartley, F., Jupiter, SD. (2016). Periodically harvested closures require full protection of vulnerable species and longer closure periods. *Biological Conservation*, **203**, 67–74.

Golden, C.D., Allison, E.H., Cheung, W.W.L., Dey, M.M., Halpern, B.S., McCauley, D.J., Smith, M., Vaitla, B., Zeller, D. & Myers S.S. (2016) Nutrition: Fall in fish catch threatens human health. *Nature*, **534**, 317–320.

Guidetti, P., Baiata, P., Ballesteros, E., Di Franco, A., Hereu, B., Macpherson, E., Micheli, F., Pais, A., Panzalis, P., Rosenberg, A.A., Zabala, M. & Sala, E. (2014) Large-Scale Assessment of Mediterranean Marine Protected Areas Effects on Fish Assemblages. *Plos One*, **9**, e91841.

Guizien, K., Belharet, M., Moritz, C. & Guarini, J.M. (2014) Vulnerability of marine benthic metapopulations: implications of spatially structured connectivity for conservation practice in the Gulf of Lions (NW Mediterranean Sea). *Diversity and Distributions*, **20**, 1392–1402.

411 Halpern, B.S. & Warner, R.R. (2003) Review Paper. Matching marine reserve design to reserve
412 objectives. *Proceedings of the Royal Society of London. Series B: Biological Sciences*, **270**,
413 1871–1878.

414 Halpern, B.S., Lester, S.E. & McLeod, K.L. (2010) Placing marine protected areas onto the
415 ecosystem-based management seascape. *Proceedings of the National Academy of Sciences*,
416 **107**, 18314–18317.

417 Harmelin, J.-G. & Harmelin-Vivien, M. (1999) A review on habitat, diet and growth of the
418 dusky grouper *Epinephelus marginatus* (Lowe, 1834). *Marine Life*, **9**, 11–20.

419 Hilborn, R. & Ovando, D. (2014) Reflections on the success of traditional fisheries
420 management. *ICES Journal of Marine Science*, **71**, 1040–1046.

421 Hilborn, R. (2015) Marine Protected Areas miss the boat. *Science*, **350**, 1326.

422 Hoggarth, D.D. (ed). (2006) *Stock Assessment for Fishery Management: A Framework Guide*
423 *to the Stock Assessment Tools of the Fisheries Management Science Programme*. Food and
424 Agriculture Organization of the United Nations, Rome.

425 Horta e Costa, B., Claudet, J., Franco, G., Erzini, K., Caro, A., Gonçalves, E.J. (2016) A
426 Regulation-Based Classification System for Marine Protected Areas (MPAs). *Marine*
427 *Policy*, **72**, 192–198.

428 Hughes, T.P., Cameron, D.S., Chin, A., Connolly, S.R., Day, J.C., Jones, G.P., McCook, L.,
429 McGinnity, P., Mumby, P.J., Pears, R.J., Pressey, R.L., Russ, G.R., Tanzer, J., Tobin, A. &
430 Young, M. a. L. (2016) A critique of claims for negative impacts of Marine Protected Areas
431 on fisheries. *Ecological Applications*, **26**, 637–641.

432 Klein, C.J., Tulloch, V.J., Halpern, B.S., Selkoe, K.A., Watts, M.E., Steinback, C., Scholz, A.
433 & Possingham, H. (2013) Tradeoffs in marine reserve design: habitat condition,
434 representation, and socioeconomic costs. *Conservation Letters*, **6**, 324–332.

435 La Mesa, G., Molinari, A., Bava, S., Finoia, M.G., Cattaneo-Vietti, R. & Tunesi, L. (2011)
436 Gradients of abundance of sea breams across the boundaries of a Mediterranean marine
437 protected area. *Fisheries Research*, **111**, 24–30.

438 Lloret, J., Biton-Porsmoguer, S., Carreño, A., Di Franco, A., Sahyoun, R., Melià, P., Claudet,
439 J., Sève, C., Ligas, A., Belharet, M., Calò, A., Carbonara, P., Coll, M., Corrales, X., Lembo,
440 G., Sartor, P., Bitetto, I., Vilas, D., Piroddi, C., Prato, G., Charbonnel, E., Bretton, O.,
441 Hartmann, V., Prats, L. & Font, T. (2019) Recreational and small-scale fisheries may pose
442 a threat to vulnerable species in coastal and offshore waters of the western Mediterranean.
443 *ICES Journal of Marine Science* (in press).

444 Melià, P. (2017) Multi-criteria Decision Making for Marine Protected Area Design and
445 Management. Pp. 125-144 in Goriup P.D. (ed.) *Management of Marine Protected Areas. A*
446 *Network Perspective from the Mediterranean and Black Seas*. John Wiley & Sons, Ltd.

447 Melià, P., Schiavina, M., Rossetto, M., Gatto, M., Fraschetti, S. & Casagrandi, R. (2016)
448 Looking for hotspots of marine metacommunity connectivity: a methodological framework.
449 *Scientific Reports*, **6**, 23705.

Neubauer, P., Jensen, O.P., Hutchings, J.A. & Baum, J.K. (2013) Resilience and recovery of overexploited marine populations. *Science*, **340**, 347–349.

Ortuño Crespo, G. & Dunn, D.C. (2017) A review of the impacts of fisheries on open-ocean ecosystems. *ICES Journal of Marine Science*, **74**, 2283–2297.

Pascual, M., Rossetto, M., Ojea, E., Milchakova, N., Giakoumi, S., Kark, S., Korolesova, D. & Melià, P. (2016) Socioeconomic impacts of marine protected areas in the Mediterranean and Black Seas. *Ocean & Coastal Management*, **133**, 1–10.

Populus, J., Vasquez, M., Albrecht, J., Manca, E., Agnesi, S., Al Hamdani, Z., Andersen, J., Annunziatellis, A., Bekkby, T., Bruschi, A., Doncheva, V., Drakopoulou, V., Duncan, G., Inghilesi, R., Kyriakidou, C., Lalli, F., Lillis, H., Mo, G., Muresan, M., Salomidi, M., Sakellariou, D., Simboura, M., Teaca, A., Tezcan, D., Todorova, V. & Tunesi, L. (2017) *EUSeaMap. A European Broad-Scale Seabed Habitat Map*. Ifremer.

Pujolar, J.M., Schiavina, M., Di Franco, A., Melià, P., Guidetti, P., Gatto, M., De Leo, G.A. & Zane, L. (2013) Understanding the effectiveness of marine protected areas using genetic connectivity patterns and Lagrangian simulations. *Diversity and Distributions*, **19**, 1531–1542.

Russ, G.R., Alcala, A.C., Maypa, A.P., Calumpong, H.P. & White, A.T. (2004) Marine reserves benefit local fisheries. *Ecological Applications*, **14**, 597–606.

Sala, E., Ballesteros, E., Dendrinos, P., Di Franco, A., Ferretti, F., Foley, D., Fraschetti, S., Friedlander, A., Garrabou, J., Güçlüsoy, H., Guidetti, P., Halpern, B.S., Hereu, B., Karamanlidis, A.A., Kizilkaya, Z., Macpherson, E., Mangialajo, L., Mariani, S., Micheli, F., Pais, A., Riser, K., Rosenberg, A.A., Sales, M., Selkoe, K.A., Starr, R., Tomas, F. & Zabala, M. (2012) The Structure of Mediterranean Rocky Reef Ecosystems across Environmental and Human Gradients, and Conservation Implications. *Plos One*, **7**, e32742.

Treml, E.A., Ford, J.R., Black, K.P. & Swearer, S.E. (2015) Identifying the key biophysical drivers, connectivity outcomes, and metapopulation consequences of larval dispersal in the sea. *Movement Ecology*, **3**, 17.

Watson, J.R., Kendall, B.E., Siegel, D.A. & Mitarai, S. (2012) Changing seascapes, stochastic connectivity, and marine metapopulation dynamics. *The American Naturalist*, **180**, 99–112.

Worm, B., Hilborn, R., Baum, J.K., Branch, T.A., Collie, J.S., Costello, C., Fogarty, M.J., Fulton, E.A., Hutchings, J.A. & Jennings, S. (2009) Rebuilding global fisheries. *Science*, **325**, 578–585.

Zupan, M., Fragkopoulou, E., Claudet, J., Erzini, K., Horta e Costa, B. & Gonçalves, E. (2018) Marine partially protected areas: drivers of ecological effectiveness. *Frontiers in Ecology and the Environment*, **16**, 381–387.

Figure legends

Figure 1. Study area and spatial distribution of suitable habitat in each of the 949 model cells considered in this study.

Figure 2. Stock biomass and catch of the three studied species (colour coded) as functions of fishing mortality rate F. Biomass and catch values (averaged over the last 10 years of a 50-years simulation) are normalized with respect to baseline values for each species (obtained at current fishing mortality rate, F_0). F was varied by applying different multipliers to the baseline, namely: 0, 0.1, 0.2, 0.25, 0.33, 0.5, 0.625, 0.75, 1, 1.5, 2, 3, 4, and 5. Maximum Sustainable Yield for each species and the corresponding values of stock biomass (B_{MSY}) are pointed out by coloured dots near the axes, while the corresponding levels of fishing mortality (F_{MSY}) are indicated by black-bordered circles. The white, black-bordered circle identifies the baseline scenario.

Figure 3. Temporal dynamics of (A) stock biomass and (B) catch for the three studied species under a MSY management (i.e., with fishing mortality rate set to F_{MSY}). Biomasses are normalized with respect to B_{MSY}, while catches are normalized with respect to their estimated current value C_0.

Figure 4. Stock biomass and catch of the three studied species as functions of the percent coverage of fully protected areas within existing MPAs. Biomass and catch values (averaged over the last 10 years of a 50-years simulation) are normalized with respect to baseline values for each species (obtained by setting the proportion of fully protected areas over the overall size of MPAs to its present value, A_0). The white, black-bordered circle identifies the baseline scenario.

510

511 **Figure 5.** Percent change of the total value of catch (compared to its present value) as a function
512 of (A) fishing mortality rate and (B) percent coverage of fully protected areas within existing
513 MPAs.

514

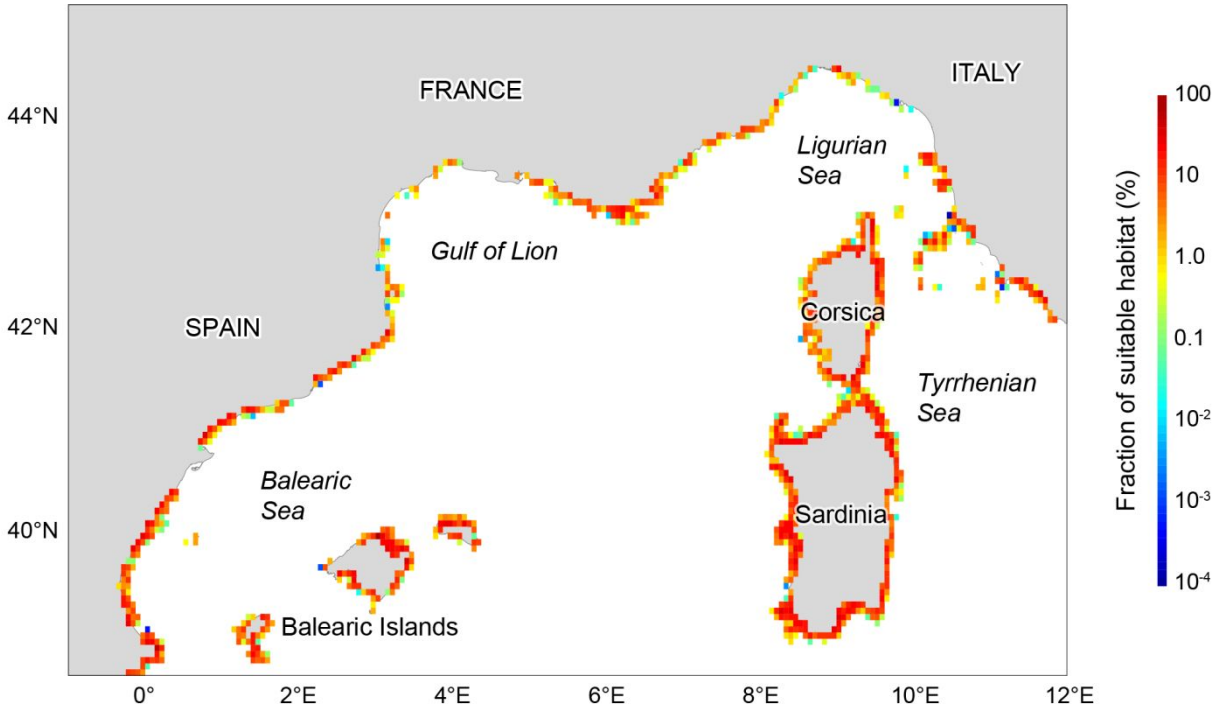

515

516 **Fig. 1**

517

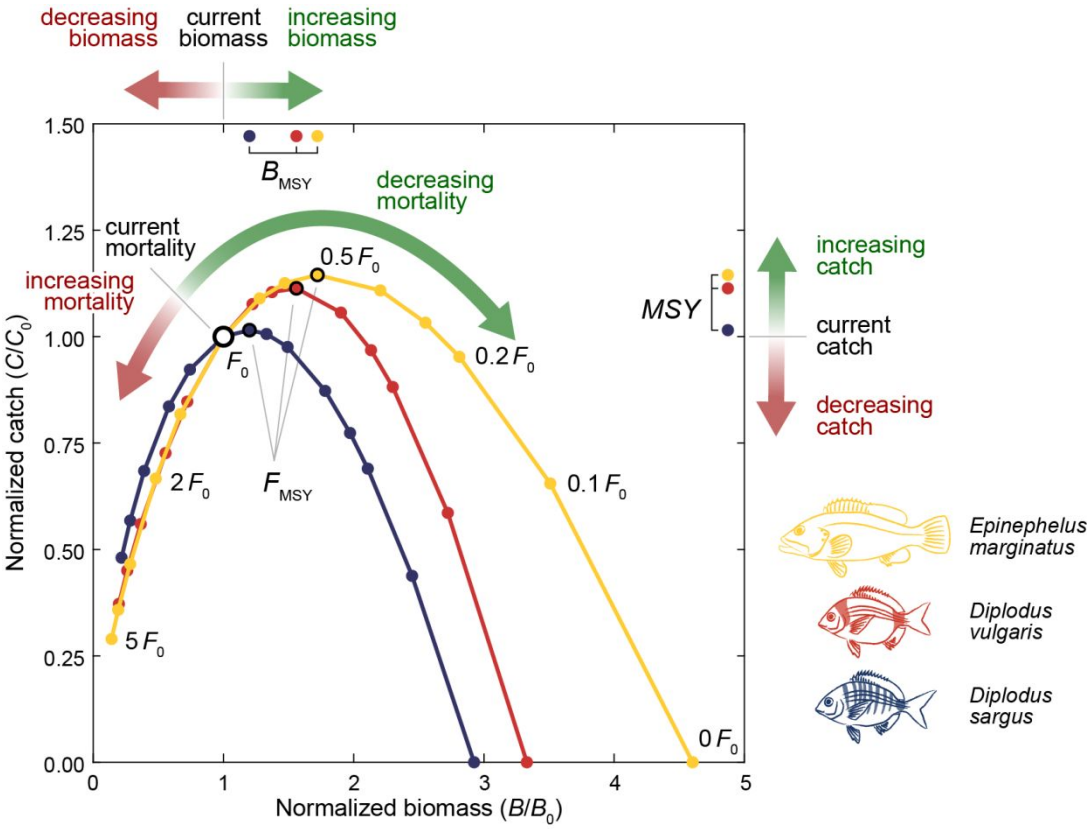

518

519 **Fig. 2**

520

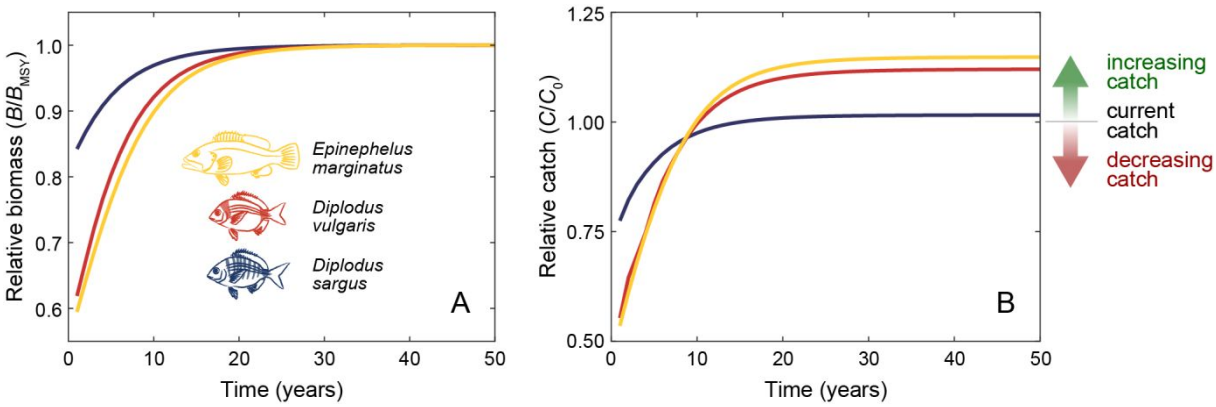

521

522 **Fig. 3**

523

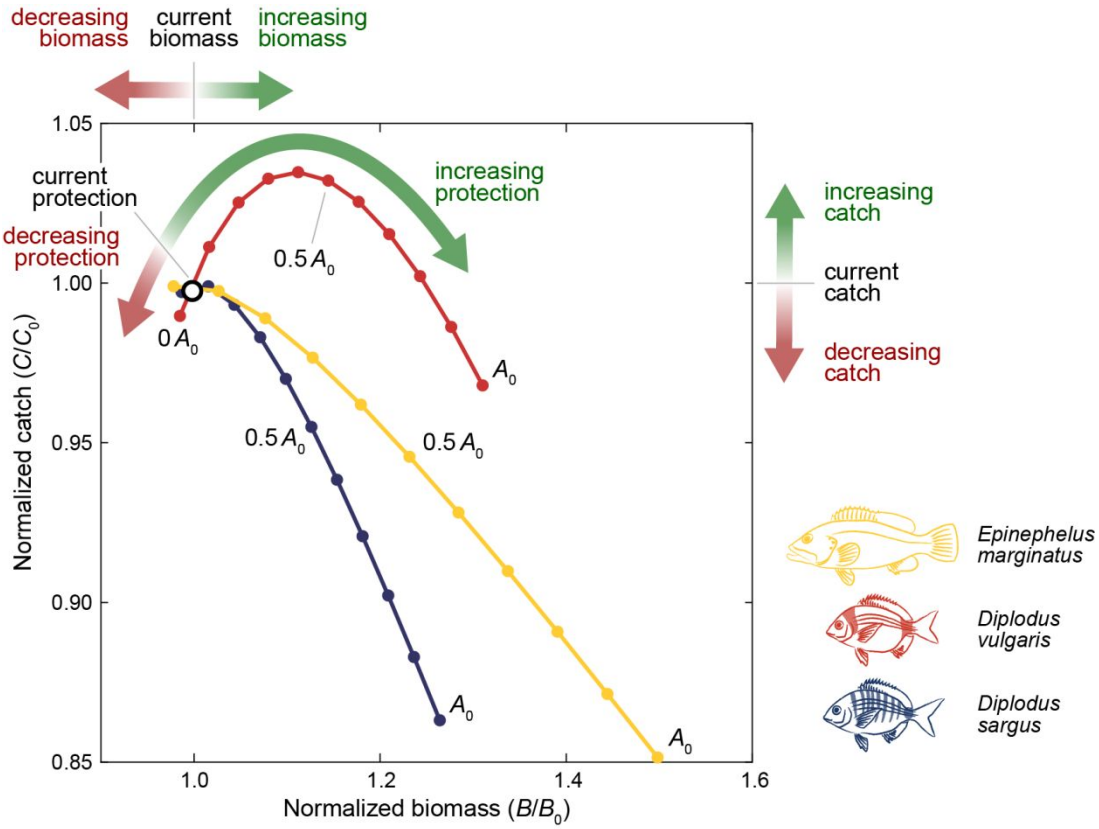

524

525 **Fig. 4**

526

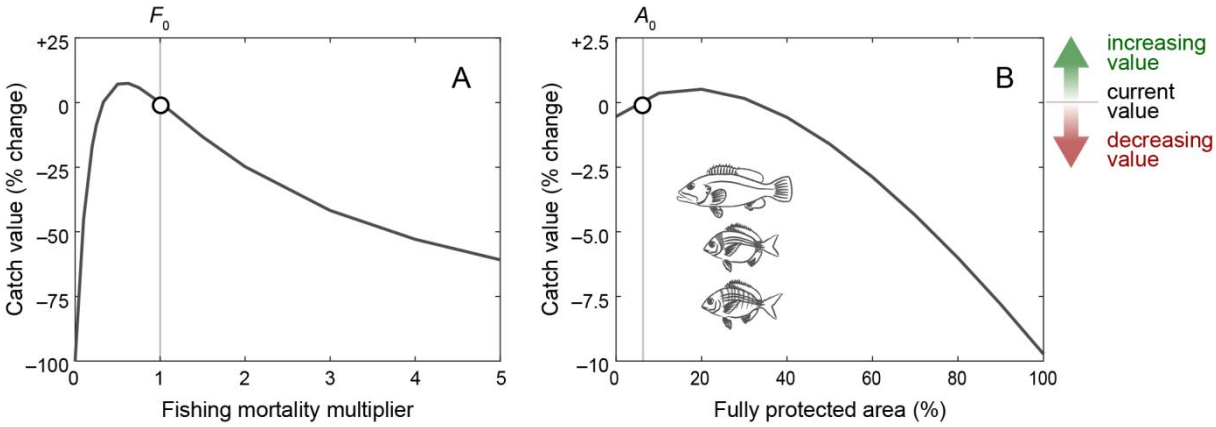
F_0
+25
0
−25
−50
−75
−100
Catch value (% change)
A
0
1
2
3
4
5
Fishing mortality multiplier
A_0
+2.5
0
−2.5
−5.0
−7.5
−10
Catch value (% change)
B
0
20
40
60
80
100
Fully protected area (%)
increasing value
current value
decreasing value

527

528 **Fig. 5**

Supplementary Information

Extending full protection inside existing multiple-use marine protected areas or reducing fishing effort outside can both deliver conservation and fisheries outcomes

Mokrane Belharet[1], Antonio Di Franco[2,3], Antonio Calò[2,4,5], Lorenzo Mari[1], Joachim Claudet[6], Renato Casagrandi[1], Marino Gatto[1], Josep Lloret[7], Charlotte Sève[6], Paolo Guidetti[2], Paco Melià[1]

[1]Dipartimento di Elettronica, Informazione e Bioingegneria, Politecnico di Milano, Via Ponzio 34/5, 20133 Milano, Italy.

[2]Université Côte d'Azur, CNRS, UMR 7035 ECOSEAS, Parc Valrose 28, Avenue Valrose, 06108 Nice, France.

[3]Stazione Zoologica "Anton Dohrn" sede interdipartimentale di Palermo, Italy

[4]CoNISMa, Piazzale Flaminio 9, 00196 Roma, Italy.

[5]Dipartimento di Scienze della Terra e del Mare (DiSTeM), Università di Palermo, Via Archirafi 20, 90123 Palermo, Italy

[6]National Center for Scientific Research, PSL Université Paris, CRIOBE, USR3278 CNRS-EPHE-UPVD, Maison des Océans, 195 rue Saint-Jacques 75005 Paris, France.

[7]University of Girona, Faculty of Science, C/Maria Aurèlia Company 69, 17003 Girona, Catalonia, Spain.

Correspondence

Mokrane Belharet

E-mail: mokrane.belharet@gmail.com

Paco Melià

E-mail: paco.melia@polimi.it

S1. Species life cycle

The three studied species have a bipartite life cycle, characterized by a pelagic phase encompassing the early life stages followed by a benthic phase for juveniles and adults. During the spawning period, eggs and larvae are released to the water column and are therefore subject to transport by marine currents, leading to the exchange of larvae among the different local populations (connectivity). At the end of the Pelagic Larval Duration (PLD), competent larvae reach suitable habitats and settle, before recruiting to the adult fraction of the population few months later (Fig. S1).

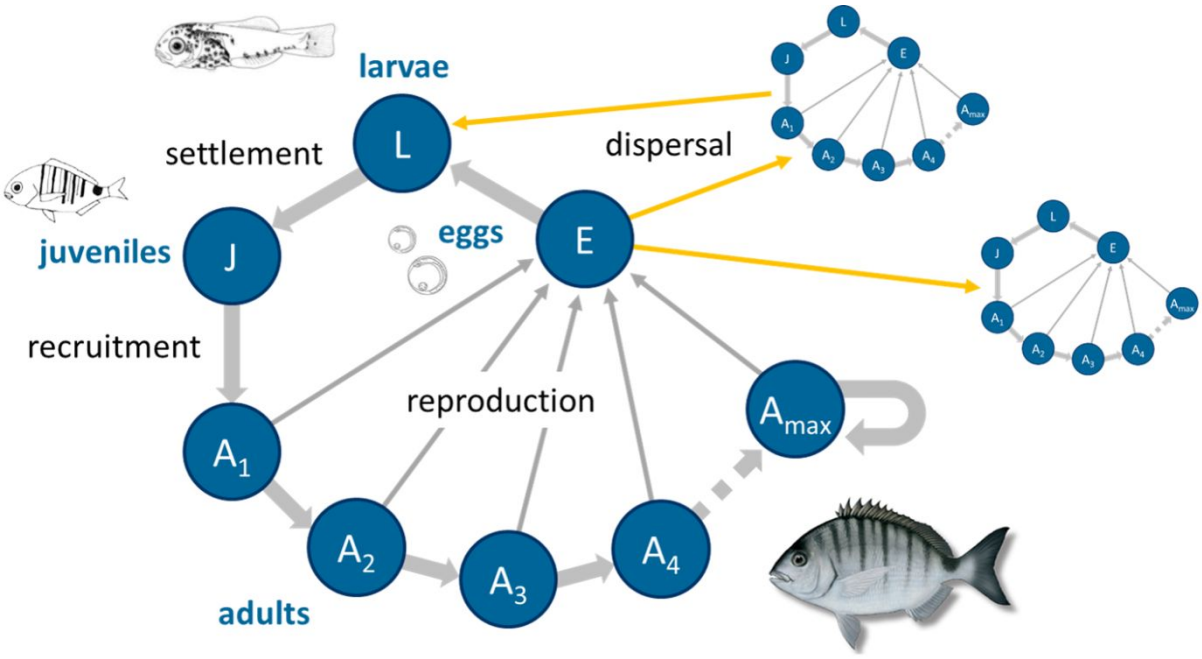

Fig. S1. Bentho-pelagic life cycle of the studied species, showing the main processes influencing metapopulation dynamics. A_1, A_2, A_3, A_4, … A_{max} are adult age classes.

S2. Data collection

Data on population density and body size of the three fish species were collected via underwater visual census (UVC) along four replicate instantaneous strip transects of 25×5 m at each site. UVC were performed on rocky substrates where other substrate types, like sand or seagrasses, generally represented less than 10% in cover (both within and around transects). Along each transect, the diver swam one way at constant speed (approximately 4 meters/min), identifying and recording the number and size of each fish encountered. Fish size (total length, TL) was recorded within 2-cm size classes for *Diplodus vulgaris* and *D. sargus*, and within 5-cm size classes for *Epinephelus marginatus*. Fish wet weight was estimated from size data by means of length-weight relationships from the available literature, while size data were converted into ages by inverting the body growth function (see section S3.1). Surveys were performed at different sampling sites located across the north-western Mediterranean Sea in June–July 2017, and at three protection levels: fully protected (no-take zone), partially protected (buffer zone) and unprotected (outside MPAs).

A long-term time series was available from Tavolara MPA (Sardinia, Italy), where data have been collected between 2005 and 2016. Samplings were carried out one or two times per year. In the latter case, the mean value of the two counts was considered. Data were collected at four protection levels: A zone (fully protected), B zone (partially protected), C zone (partially protected) and control zone outside the MPA (unprotected). For each zone, two locations (5 to 10 km from each other) were chosen. In each location, two sites (~100 m from each other) were randomly selected, where four replicates (i.e. UVC transects) were performed at two different depth intervals (5–10 m and 12–18 m). Therefore, for each zone, a total of eight replicates were considered (the two depth intervals were pooled).

S3. Model description

The model takes into account all the key biological processes characterizing the species life-history, such as reproduction, larval dispersal, recruitment, as well as natural and fishing mortality, which are described in detail in the following sections.

S3.1. Body growth

Body size is a primary determinant of most biological traits in fishes. Hence, we used a body growth model to link fish age to the remaining vital traits. We described body length as a function of age a with a von Bertalanffy function:

$$L(a) = L_{\infty}(1 - \exp\left(-k(a - a_0)\right))$$

where L_{∞} is the asymptotic body length, k is the Brody coefficient and a_0 is the constant that determines the hypothetical age at length zero. Parameter values for the three studied species were derived from the literature and are reported in Table S1.

S3.2. Reproduction

S3.2.1. Maturity

The fraction m of mature individuals in the population was expressed as a function of body length L using the relationship reported by Goncalves and Erzini (2000):

$$m = \frac{1}{1 + \exp\left(-\alpha_m(L - \beta_m)\right)}$$

where α_m and β_m are species-specific constants whose values were gathered from the literature (see Table S1).

S3.2.2. Fecundity

Fecundity f, defined as the number of eggs released by a mature female during the spawning season, was linked to body length L of females via an allometric relationship:

$$f = \alpha_f L^{\beta_f}$$

where the constants α_f and β_f were estimated by fitting length-fecundity data for *D. sargus* and *D. vulgaris* (Di Franco, manuscript in preparation). In the case of E. *marginatus* we used the parameters reported by Reñones *et al*. (2010) for the same species in the Mediterranean Sea (see Table S1).

S3.2.3. Sex determination

Sex ratio at age a, $SR(a)$, defined here as the proportion of females in the cohort of fish aged a, was also linked to age through body length. For *D. vulgaris* and *E. marginatus*, it was estimated using the following relationship:

$$SR = \alpha_{SR} + \frac{\beta_{SR}}{1 + \exp\left(-\gamma_{SR}(L - \delta_{SR})\right)}$$

For *E. marginatus* , parameters α_{SR}, β_{SR}, γ_{SR} and δ_{SR} were taken from the literature (Reñones *et al.* 2010), while for *D. vulgaris* they were calibrated by fitting the length frequency distribution of females reported by Taieb *et al*. (2012). For *D. sargus*, constant values were used for different length intervals according to the data reported by Mouine *et al*. (2007) and Benchalel & Kara (2013). Parameter values are reported in Table S1.

S3.2.4. Egg production

The total number of eggs produced in each cell depends upon abundance, sex ratio, maturity and fecundity of adult fish. These variables can change as a consequence of protection level. Therefore, for each cell we calculated the area associated to the different protection levels. The total number of eggs produced in cell *i* in year *t* was calculated as

$$N^E_{\{i,t\}} = A_i^{SH} \sum_p \sum_a D_{\{a,i,p,t\}} m(a) f(a) SR(a) \varphi_{\{p,i\}}$$

where A_i^{SH} is the extent of suitable habitat in cell *i*; p is the protection level (fully protected, partially protected, unprotected); a is fish age (from 1 to $a_{\max}$); $D_{\{a,i,p,t\}}$ is the density of fish aged a in cell *i*, subject to protection level p at time *t*; $m(a)$, $f(a)$, and $SR(a)$ are maturity,

fecundity and sex ratio of age class a, respectively; and $\varphi_{\{p,i\}}$ is the fraction of cell *i* associated with protection level *p*.

S3.3. Larval dispersal

During the spawning period, eggs and larvae produced by each local population (i.e. associated to a specific cell) are released into the water column, where they are subject to transport by marine currents throughout their PLD. To estimate the proportion of larvae exchanged among the different cells of our study area, we simulated larval dispersal for the three studied species using a biophysical model.

The physical component of the Lagrangian model was based on daily average current velocity fields obtained from the Mediterranean Sea physics reanalysis (Fratianni *et al.* 2014), which are provided at a 1/16° (~6-7 km) horizontal resolution and 72 unevenly spaced vertical levels. Lagrangian particles were dispersed as horizontal, two-dimensional passive drifters. The vertical component of current velocity fields was not considered, since horizontal velocities are several orders of magnitude higher than vertical ones (d'Ovidio *et al.* 2004; Rossi *et al.* 2014). The time step of the simulations was set to 3h and was determined (on the basis of the grid cell size and the currents' maximum velocity) so that larvae do not cross more than one cell boundary in a single time step.

We released and subsequently tracked 10 particles from each sub-cell of the bathymetric grid (see main text), hence 9000 for each cell. The initial longitude and latitude of the particles were randomly assigned within each originating sub-cell, while their depths were evenly spaced along the vertical axis within a 0-50 m depth interval. We assigned to each released particle two species-specific parameters, namely the release date and the PLD, which were randomly drawn from Gaussian distributions whose average and standard deviation are listed in Table S2. For each species, the release timing was set so as to match the spawning season.

At the end of the simulations, for each species and each year we calculated a connectivity matrix, whose element $c_{\{i,j,t\}} = \frac{n_{i\to j,t}}{n_{i,t}}$ is the ratio between $n_{i\to j,t}$ (i.e. the number of larvae starting from source cell *i* and successfully arriving to destination cell *j* at the end of their PLD in year *t*) and $n_{i,t}$ (i.e. the total number of propagules released from cell *i* in year *t*). The diagonal elements of the connectivity matrix represent the retention rate of the considered cells.

Species-specific connectivity matrices averaged over the period 2004–2015 are shown in Fig S2. To facilitate the reading of the matrices, the study area was subdivided into 12 different regions taking into account the coastal morphology and the continuity of the suitable habitat.

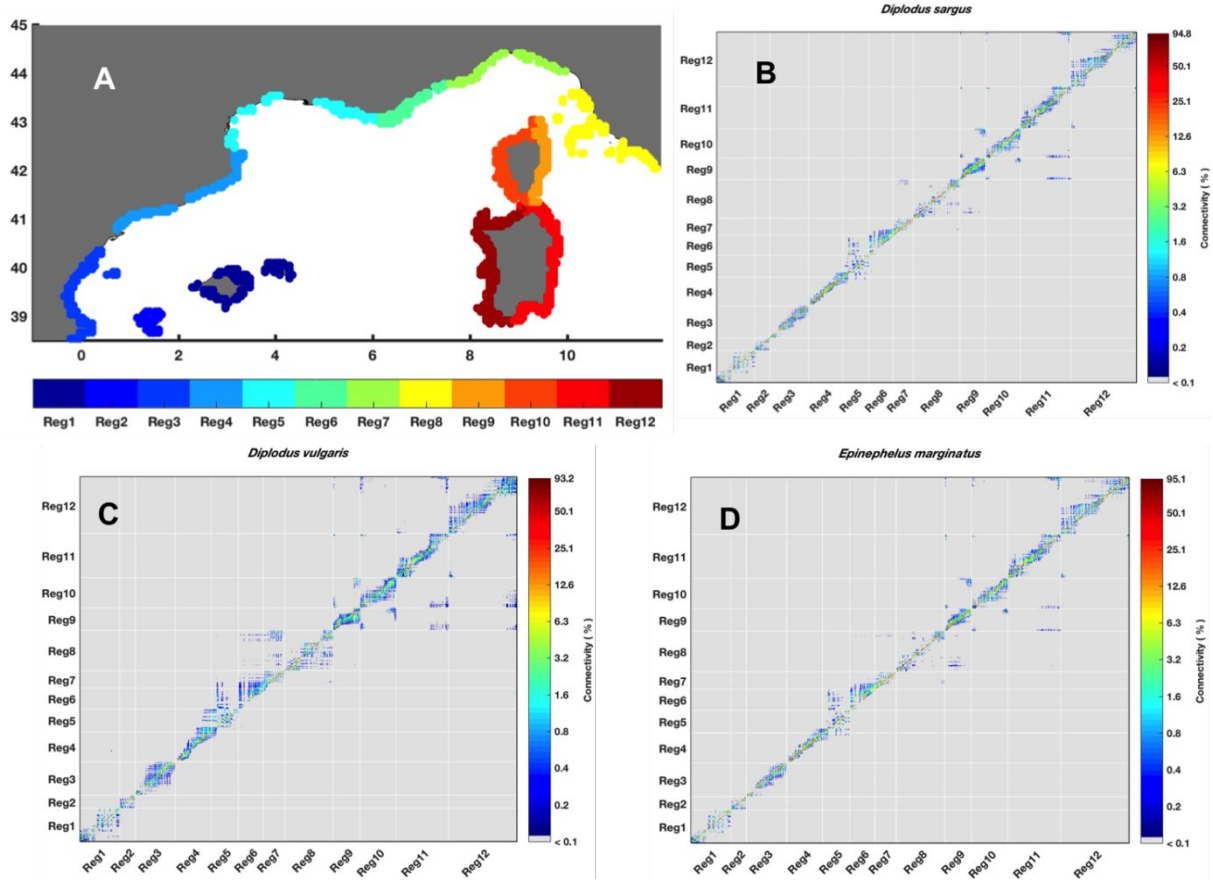

Fig. S2. Time-averaged connectivity matrices estimated for the three studied species: *D.sargus* (B), *D.vulgaris* (C) and *E.marginatus* (D) using the results of Lagrangian simulations. To facilitate reading, the connectivity matrices are divided into 12 regions as represented in panel (A). The matrix rows refer to the release sites, while the columns represent the destination sites of the settled larvae. Colours indicate the time-averaged probability $\bar{c}_{\{i,j\}}$ that a larva born in site *i* (row) is transported to site *j* (column).

The results show that, out of 949×949 = 900 601 possible connections, connectance (here defined as the number of connections with time-averaged $\bar{c}_{\{i,j\}} \geq 0.1\%$) is about 1.48% for *D.sargus*, 2.15% for *D.vulgaris*, and 1.55% for *E.marginatus*. The relatively high value found for *D.vulgaris* can be ascribed to its longer PLD. The average connectivity scores range between 0–86% for *D.sargus*, 0–93% for *D.vulgaris*, and 0–83% in the case of *E.marginatus*. Overall, the connectivity matrices show high local retention rates for the three studied species. However, the spatial median of the retention rate of *D.vulgaris* (~6%) is much lower than that of *E.marginatus* (~15%) and *D.sargus* (16%). Connectance and self-retention appear to be directly and inversely proportional, respectively, to the species-specific PLDs.

The dispersal kernels shown in Fig S3 display the frequency distributions of the distances travelled by the simulated Lagrangian particles. The results show that the mode of the frequency distribution, including all successful dispersal particles (i.e. those reaching a cell with suitability >0), is located between 0–5 km from the spawning source for *D. sargus* and *E. marginatus*, whereas it is located between 5–10 km in the case of *D. vulgaris*. Dispersal patterns decline with increasing distance past the mode of the distributions. The median dispersal distance is about 8.21 km for *D.sargus*, 16.58 km for *D. vulgaris* and 8.50 for *E. marginatus,* whereas the maximum travelled distances are approximately 80 km, 180 km, and 115 km, respectively. Overall, ~55–60% of the Lagrangian particles reached cells with suitability ≥5%, ~30% reached cells with suitability ≥10%, and ~6–7% reached cells with suitability ≥20%.

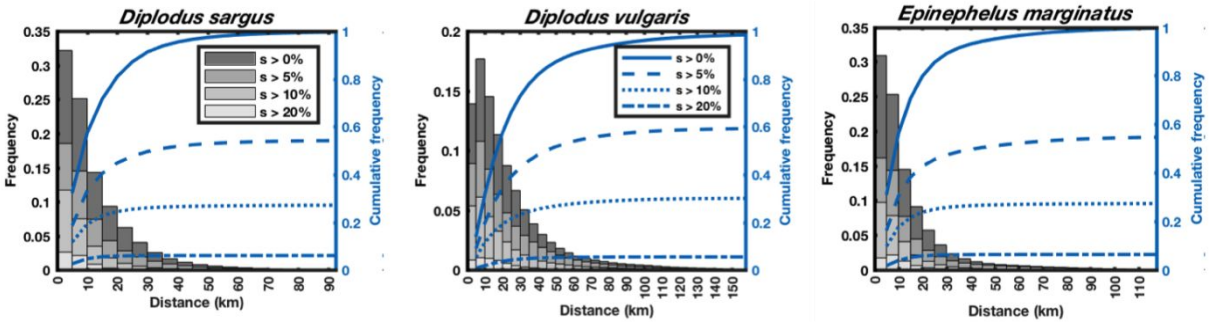

Fig. S3. Dispersal kernels of the three studied species. For each species, four superimposed histograms indicate the fraction of particles whose final positions had a suitability ≥0%, 5%, 10% and 20%, respectively. Each histogram is associated with its cumulative frequency, which represents the cumulative sum of the frequency distributions.

S3.4. Settlement

At the end of the PLD, the number of competent larvae settling at cell *i* in year *t* depends on the number of eggs produced in the different cells making up the metapopulation as well as on connectivity. It can be expressed as

$$N^{L}_{\{i,t\}} = \sum_{j=1}^{949} N^{E}_{\{j,t\}}\, c_{\{j,i,t\}}$$

Where $N^{E}_{\{j,t\}}$ is the number of eggs produced in cell *j* at time *t*, and $c_{\{j,i,t\}}$ is the fraction of propagules released from cell *j* and reaching cell *i*. Therefore, the density of new settlers in cell *i* at time *t* was evaluated as the ratio between the total number of settlers and the surface area of the cell, $D^{L}_{\{i,t\}} = \frac{N^{E}_{\{i,t\}}}{A_i}$.

S3.5. Recruitment

New settlers recruiting into a new cohort are assumed to experience density-dependent mortality following a Beverton–Holt relationship. The density of new recruits was therefore expressed as follows:

$$D^{R}_{\{i,t\}} = D^{L}_{\{i,t\}} \frac{R_{\max}}{D^{L}_{\{i,t\}} + gR_{\max}}$$

Where $D^{L}_{\{i,t\}}$ is the density of settlers, and $R_{\max}$ and g are species-specific parameters describing the maximum recruitment rate and the intensity of density dependence on recruitment, respectively. Parameter values are reported in Table S1.

S3.6. Mortality

S3.6.1. Natural mortality

Natural mortality rate was estimated using the age-frequency distribution method (Sparre *et al.* 1998). Under the assumption of population stationarity, mortality rate can be derived by fitting the exponentially declining frequency of older age groups in the population. Therefore, the mortality rate is estimated as the slope of the linearized age-frequency curve, i.e the graphical representation of the logarithms of fish abundance plotted against age. In the absence of more specific information, natural mortality rate was assumed to be constant across space and time. It was evaluated as the mean value of the natural mortality rates calculated at different locations by using size-frequency data from local populations inside fully protected areas of the MPAs. Size-structured data were converted into age-structured data using the body growth curve reported below. The estimated values of natural mortality rate at different locations are listed in Table S3.

S3.6.2. Fishing mortality

For the purpose of this study, we assumed fishing mortality rates to be constant over time. However, we considered three different fishing mortality rates for Spain (F_{SP}) , France (F_{FR}) and Italy (F_{IT}) for each species. This choice was motivated by the fact that fisheries management policies are generally different from one country to another. Due to the lack of accurate information about the fishing mortality rates of the three studied species, those parameters were estimated via model calibration.

The minimum landing size established by the Council Regulation No. 1967/2006 for the three studied species is 23 cm for *D. sargus*, 18 cm for *D. vulgaris* and 45 cm for *E. marginatus*.

These body sizes correspond approximately to age-class 3 for all three studied species. However, individuals of smaller size are also caught, and are sometimes available in the fish markets. For these reasons and for the sake of simplicity, we assumed the following age-dependent selectivity:

$$F(a) = \begin{cases} 0 & \text{if } a = 1 \\ 0.5F & \text{if } a = 2 \\ F & \text{if } a \geq 3 \end{cases}$$

with F being the calibrated value of the fishing mortality rate.

S3.7. Metapopulation dynamics

In each cell, and –within a given cell– in each sub-cell characterized by a specific protection level, population dynamics were described by an age-structured model with a time step of 1 year. Abundance of each age class was expressed in terms of population density, where the generic state variable $D_{\{a,i,p,t\}}$ represents the density (ind. m^{-2}) of fish of age a (= 1, 2, ... $a_{\max}$) in a sub-area of cell i (= 1, 2, ... 949) characterized by protection level p (= fully protected, partially protected, unprotected) at time t.

The first age class takes recruitment (assumed to be distributed homogeneously across the whole cell) as an input, while the abundance of the other age classes depends upon survival during the transition from an age class to the following:

$$D_{\{1,i,p,t+1\}} = D^R_{\{i,t\}} \exp\left(-Z_{\{0,i,p\}}\right) \quad \text{if } a = 0$$

$$D_{\{a+1,i,p,t+1\}} = D_{\{a,i,p,t\}} \exp\left(-Z_{\{a,i,p\}}\right) \quad \text{if } 1 \leq a < a_{\max} - 1$$

$$D_{\{a_{\max},i,p,t+1\}} = D_{\{a_{\max}-1,i,p,t\}} \exp\left(-Z_{\{a_{\max}-1,i,p\}}\right) + D_{\{a_{\max},i,p,t\}} \exp\left(-Z_{\{a_{\max},i,p\}}\right) \text{ otherwise}$$

where $D^R_{\{i,t\}}$ is the density of recruits in cell i at time t, and Z is the total mortality rate.

Stock biomass in cell i at time t can be calculated from the density of all age classes over the different protection levels by means of the following equation:

$$B_{\{i,t\}} = A_i^{SH} \sum_p \sum_a D_{\{a,i,p,t\}} W(a) \varphi_{\{p,i\}}$$

where A_i^{SH} is the extent of suitable habitat in cell *i*; *p* is the protection level (fully protected, partially protected, unprotected); *a* is fish age (from 1 to $a_{\max}$); $D_{\{a,i,p,t\}}$ is the density of fish aged *a* in cell *i*, subject to protection level *p* at time *t*; $W(a)$ is the average body mass of fish in age class a, calculated using the allometric length-weight relationship $W(a) = \alpha_W L(a)^{\beta_W}$ reported by Le Cren (1951), in which α_W and β_W are constants, and $L(a)$ is the body length (cm) of an individual of age a; and $\varphi_{\{p,i\}}$ is the fraction of cell *i* associated with protection level *p*.

Finally, total catch $C_{\{i,\,t+1\}}$ from cell *i* between time *t* and time *t* + 1 was estimated using the Baranov equation (Baranov 1945):

$$C_{\{i,t+1\}} = A_i^{SH} \sum_p \sum_a \frac{F_{\{a,i,p\}}}{Z_{\{a,i,p\}}} \left(1 - exp\left(-Z_{\{a,i,p\}}\right)\right) D_{\{a,i,p,t\}} W(a) \varphi_{\{p,i\}}$$

where, A_i^{SH} is the extent of suitable habitat in cell *i*; *p* is the protection level (fully protected, partially protected, unprotected); *a* is fish age (from 1 to $a_{\max}$); *F* and *Z* are fishing mortality rate and total mortality rate, respectively; $D_{\{a,i,p,t\}}$ is the density of fish aged *a* in cell *i*, subject to protection level *p* at time *t*; $W(a)$ is the average body mass of fish in age class a; and $\varphi_{\{p,i\}}$ is the fraction of cell *i* associated with protection level *p*.

S4. Model calibration and validation

The model was calibrated against data about the spatial distribution of the three species, collected in 2017 across the study area (see section S2). Data from replicated transects collected in the same location and in the same year were averaged to obtain a single estimate of population density for each location. We used two thirds of the data collected in unprotected areas for calibration, while the remaining third of the data from unprotected areas was used for validation (see below). Specifically, we found the parameter set minimizing the residual sum of squares (RSS) between the predicted and observed densities at different locations. To this end, we solved the following optimization problem:

$$\min_{\underline{\theta}} \sum_k \left(\bar{y}_k^{\text{obs}} - \hat{y}_k^{\text{mod}}\right)^2$$

where $\underline{\theta}$ is the parameter set to be estimated, $\bar{y}_k^{\text{obs}}$ is the observed fish density (averaged over replicated transects) at location k, and $\hat{y}_k^{\text{mod}}$ is the corresponding density predicted by the model in the unprotected portion of the model cell containing that location. Five parameters ($R_{\max}$ and g from the stock-recruitment relationship, along with country-specific average fishing mortality rates F_{SP}, F_{FR} and F_{IT}) were calibrated for each species.

To assess model performances in reconstructing observed patterns of population density in space and time, we used two different datasets: (i) the time series of population density for the three species, collected in the partially and fully protected areas of the Tavolara MPA, as well as in nearby unprotected areas, between 2005–2016, and (ii) the population density data collected in partially and fully protected areas of the north-western Mediterranean Sea, together with the remaining third of the data collected in unprotected areas.

Fig. S4 shows a comparison between observed and predicted fish density across the study area. In broad terms, model predictions seem in good agreement with field observations. The median values of predicted density, evaluated over the whole spatial domain, are 0.032 ind. m^{-2} for *D.*

sargus, 0.053 ind. m^{-2} for *D. vulgaris* and 0.002 ind. m^{-2} for *E. marginatus*, respectively, and are almost identical to the median values of observed density, which are 0.032 ind. m^{-2}, 0.055 ind. m^{-2} and 0.002 ind. m^{-2}, respectively. This matching between observed and predicted fish densities was confirmed by a Wilcoxon signed-rank test at a 5% significance level ($P >> 0.05$ for all three species).

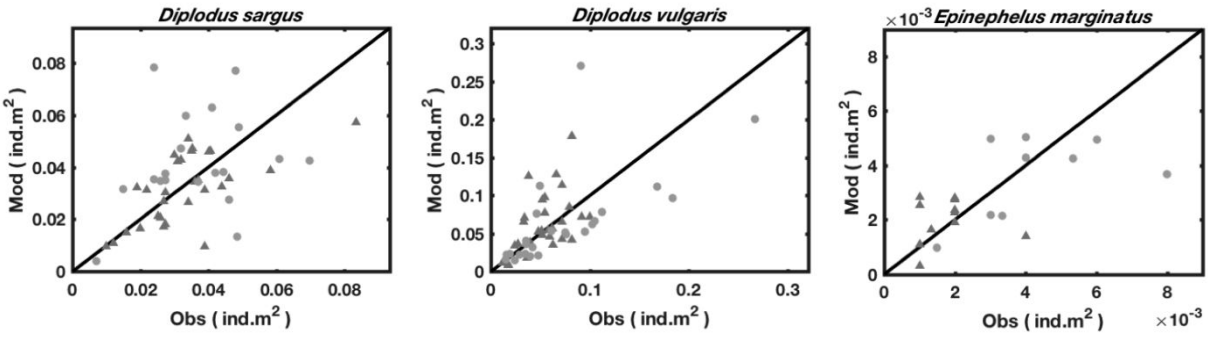

Fig. S4. Observed (Obs) vs. predicted (Mod) total population density of the three studied species. Observations were collected in 2017 at different locations within the study area. Triangles indicate data used for calibration, whereas circles indicate those used for validation.

Fig. S5 shows the ability of the model to simulate the population dynamics of the three species over time, by comparing observed and predicted population densities in the Tavolara MPA between 2004–2016. Again, predictions seem in good agreement with observations. The ratio of observed on predicted density is 0.72 for *D. sargus*, 0.94 for *D. vulgaris* and 1.06 for *E. marginatus*, respectively, in fully protected areas, 0.53/0.66/0.55 in partially protected areas, and 0.80/0.90/0.52 in the unprotected areas.

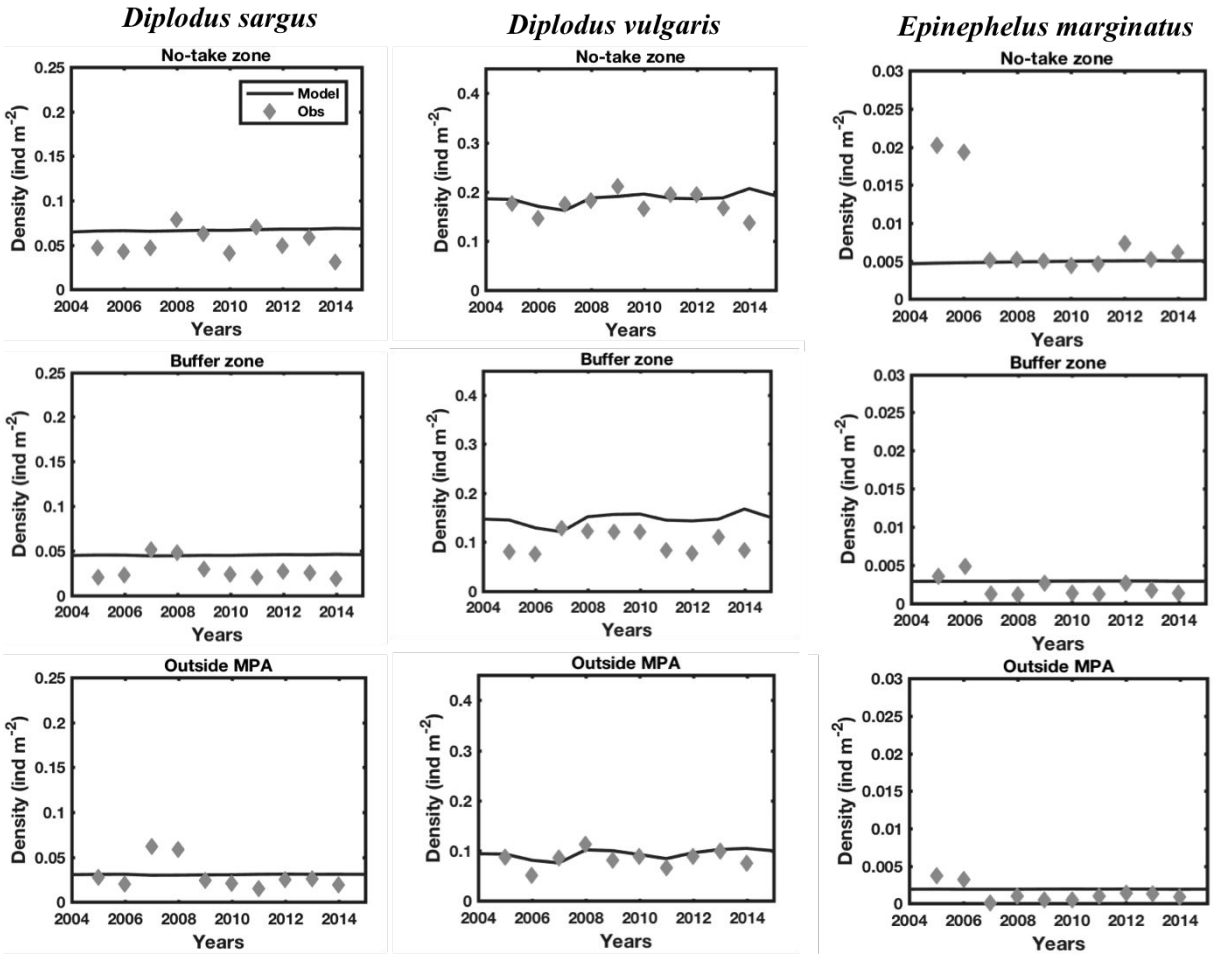

Fig. S5. Predicted population dynamics of the three studied species over the period 2004–2016 against field observations from the fully protected area (no-take zone), the partially protected area (buffer zone) and unprotected areas (outside MPA) of Tavolara MPA.

Despite a few discrepancies between specific observations and predictions, the overall ability of the model to match the observed spatiotemporal patterns of field data can be considered satisfactory. To further compare the predictive performances of the three species-specific models, we constructed a Taylor diagram (Taylor 2001), shown in Fig S6. The diagram was built using all the observed and predicted data used in both calibration and validation. The Taylor diagram allows the simultaneous assessment of the degree of similarity between observed (reference) and predicted (test) data in terms of three statistics: Pearson correlation coefficient, root mean square deviation (RMSD) and normalized standard deviation. If the models were perfect, the points indicating model predictions (labelled DS, DV, EM in the

figure) would overlap exactly the reference point (OBS). The figure indicates that the model for *D. vulgaris* has the best performances, followed by that for *D. sargus* and then by that for *E. marginatus*. In fact, although the predictions for *D. sargus* and *D. vulgaris* have almost the same normalized RMSD (0.47 vs. 0.46, respectively) and the same normalized standard deviation (1.13 and 1.15), the Pearson correlation coefficient is significantly higher for *D. vulgaris* than for *D. sargus* (0.78 vs. 0.53, $P<<0.01$). As for *E. marginatus*, although the Pearson correlation coefficient is slightly higher than that of *D. sargus* (0.57 vs. 0.53 respectively, $P<<0.01$), the normalized RMSE (0.95) is much higher and the normalized standard deviation (0.33) is farther from the reference than that for *D. sargus*.

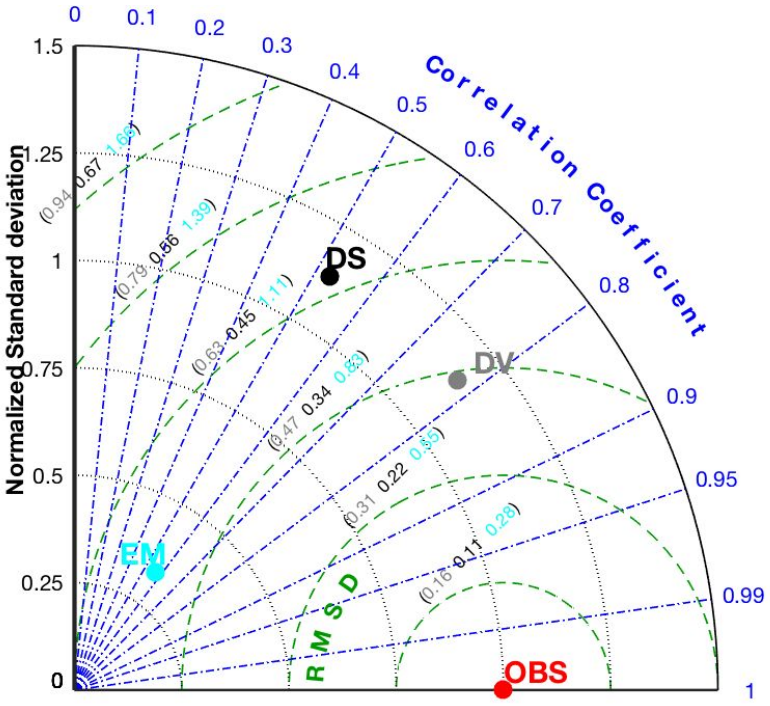

Fig. S6. Taylor diagram summarizing the comparison between field observations and model predictions of population density for the three studied species. DS: *D. sargus* (black); DV: *Diplodus vulgaris* (grey); EM: *E. marginatus* (green). RMSD values (green dashed arcs) and standard deviation values (black dotted arcs) are normalized with respect to the mean observed density of each species. Colour coded numbers between parentheses indicate RMSD values for each species.

Table S1. Species-specific parameters used in the metapopulation models for the three model species.

Function / parameters	Description	Parameter value		
		D. sargus	*D. vulgaris*	*E. marginatus*
Body growth				
L_∞	asymptotic body length (cm)	41.67	25.72	123.86
k	Brody growth coefficient (yr^{-1})	0.17	0.32	0.087
a_0	age at length zero (yr)	–0.99	–0.88	–1.02
Weight at length curve				
α_W	scale parameter ($g\ cm^{-b}$)	0.016	0.015	0.010
β_W	exponent	3.05	3.00	3.12
Fecundity at length curve				
α_f	scale parameter ($eggs\ cm^{-b_{fec}}$)	0.084	0.084	0.140
β_f	exponent	4.51	4.51	3.82
Maturity curve				
α_m	slope of the maturity curve	1.26	0.75	0.22
β_m	size at 50% maturity (cm)	20.06	18.33	49.10
Sex determination				
SR	sex ratio by body size class	0 (L<14 cm) 0.6(14≤L≤34) 1 (L>34cm)		
α_{SR}	offset of the sex ratio		0.32	0.00
β_{SR}	asymptotic sex ratio		0.40	1.00
γ_{SR}	slope of the sex ratio curve		0.31	–0.082
δ_{SR}	size at 1:1 sex ratio (cm)		15.28	79.90
Natural mortality				
M	natural mortality rate (yr^{-1})	0.26	0.38	0.21
Fishing mortality				
F_{SP}	fishing mortality rate (yr^{-1}), Spain	0.08	0.14	0.10
F_{FR}	fishing mortality rate (yr^{-1}), France	0.20	0.52	0.29
F_{IT}	fishing mortality rate (yr^{-1}), Italy	0.49	0.84	0.49
Recruitment				
R_{max}	max. recruitment rate ($ind\ m^{-2}$)	0.029×10^{-3}	0.27×10^{-3}	0.0015×10^{-3}
g	half-saturation constant	0.5	0.1	1

Table S2. Early life history traits of the three studied species used in the Lagrangian simulations.

Species	**Release period**		**PLD**		**References**
	Mean (date)	**SD** (days)	**Mean** (days)	**SD** (days)	
D. sargus	15 May	5	17	2	Macpherson *et al*. (1997); Di Franco & Guidetti (2011); Giacalone *et al*. (2018)
D. vulgaris	15 Dec.	19	41	8	Macpherson *et al*. (1997); Macpherson & Raventós (2006) ; Di Franco *et al.* (2013)
E. marginatus	1 Aug.	5	25	1.5	Zabala *et al*. (1997); Francour & Ganteaume (1999); Hereu *et al*. (2006); Macpherson & Raventós (2006); Cunha *et al*. (2009); Reñones *et al*. (2010)

Table S3. Natural mortality rates (*M*) estimated for the three studied species at different locations of the NWM using the age-frequency method. All the values of *M* listed in the table are significant at the 10% significance level ($P<0.1$). R is the correlation coefficient of the linear fitting of the logarithm abundance density versus age. The last column reports the number of age classes taken into account in the fitting process.

Species	**Latitude** (°N)	**Longitude** (°W)	***M*** (year^{-1})	**R**	**Age classes** (#)
D. sargus	40.717	17.801	0.190	–0.60	13
	43.326	5.159	0.362	–0.71	11
	43.894	15.145	0.56	–0.89	6
	41.336	9.245	0.149	–0.70	8
	41.459	9.020	0.227	–0.82	11
	42.049	3.218	0.136	–0.65	10
	42.464	3.162	0.269	–0.72	8
	40.912	9.743	0.146	–0.67	8
	41.120	8.320	0.195	–0.73	10
	44.091	9.740	0.268	–0.63	7
	44.134	9.634	0.354	–0.9	8
	44.315	9.157	0.280	–0.97	6
	40.876	9.781	0.297	–0.98	6
D. vulgaris	37.991	12.415	0.514	–0.91	4
	37.725	20.928	0.275	–0.92	4
	41.336	9.245	0.253	–0.55	7
	42.043	3.223	0.393	–0.76	5
	42.041	3.227	0.287	–0.72	5
	42.468	3.160	0.61	–0.91	6
	41.121	8.317	0.343	–0.66	6
E. marginatus	44.315	9.165	0.154	–0.79	6
	42.042	3.225	0.310	–0.95	6
	44.315	9.157	0.165	–0.91	5

Supplementary references

Baranov, F.I. (1945) *On the Question of the Biological Basis of Fisheries: On the Question of the Dynamics of the Fishing Industry*. Indiana University.

Benchalel, W. & Kara, M.H. (2013) Age, growth and reproduction of the white seabream *Diplodus sargus sargus* (Linneaus, 1758) off the eastern coast of Algeria. *Journal of Applied Ichthyology*, **29**, 64–70.

Di Franco, A. & Guidetti, P. (2011) Patterns of variability in early-life traits of fishes depend on spatial scale of analysis. *Biology Letters*, **7**, 454–456.

Di Franco, A., Qian, K., Calò, A., Lorenzo, M.D., Planes, S. & Guidetti, P. (2013) Patterns of variability in early life traits of a Mediterranean coastal fish. *Marine Ecology Progress Series*, **476**, 227–235.

Fratianni, C., Simoncelli, S., Pinardi, N., Cherchi, A., Grandi, A. & Dobricic, S. (2015). "Mediterranean RR 1955-2015 (Version 1) ". [Data set]. Copernicus Monitoring Environment Marine Service (CMEMS).

Goncalves, J.M.S. & Erzini, K. (2000) The reproductive biology of the two-banded sea bream (Diplodus vulgaris) from the southwest coast of Portugal. *Journal of Applied Ichthyology*, **16**, 110–116.

Le Cren, E.D. (1951) The Length-Weight Relationship and Seasonal Cycle in Gonad Weight and Condition in the Perch (Perca fluviatilis). *The Journal of Animal Ecology*, **20**, 201.

Mouine, N., Francour, P., Ktari, M.-H. & Chakroun-Marzouk, N. (2007) The reproductive biology of Diplodus sargus sargus in the Gulf of Tunis (central Mediterranean). *Scientia Marina*, **71**, 461–469.

d'Ovidio, F., Fernández, V., Hernández-García, E. & López, C. (2004) Mixing structures in the Mediterranean Sea from finite-size Lyapunov exponents. *Geophysical Research Letters*, **31**.

Reñones, O., Grau, A., Mas, X., Riera, F. & Saborido-Rey, F. (2010) Reproductive pattern of an exploited dusky grouper *Epinephelus marginatus* (Lowe 1834) (Pisces: Serranidae) population in the western Mediterranean. *Scientia Marina*, **74**, 523–537.

Rossi, V., Ser-Giacomi, E., López, C. & Hernández-García, E. (2014) Hydrodynamic provinces and oceanic connectivity from a transport network help designing marine reserves. *Geophysical Research Letters*, **41**, 2883–2891.

Sparre, P., Venema, S.C., DANIDA & Nations, F. and A.O. of the U. (1998) *Introduction to Tropical Fish Stock Assessment: Manual*. Food and Agriculture Organization of the United Nations.

Taieb, A.H., Ghorbel, M., Hamida, N.B.H. & Jarboui, O. (2012) Reproductive biology of Diplodus vulgaris (Teleostei, Sparidae) in the southern Tunisian waters (Central Mediterranean). *Acta Adriatica*, **53**, 437–446.

Taylor, K.E. (2001) Summarizing multiple aspects of model performance in a single diagram. *Journal of Geophysical Research: Atmospheres*, **106**, 7183–7192.